www.ietdl.org

Published in IET Control Theory and Applications
Received on 7th February 2014
Revised on 15th June 2014
Accepted on 24th July 2014
doi: 10.1049/iet-cta.2014.0138

ISSN 1751-8644

Coefficient ratios-based robust sliding surface and integral sliding mode control designs with optimal transient responses

Günyaz Ablay

Electrical-Electronics Engineering Department, Abdullah Gül University, Kayseri 38039, Turkey
E-mail: gunyaz.ablay@agu.edu.tr

Abstract: A coefficient ratio-based sliding surface algorithm and an integral sliding mode control approach are proposed for multivariable dynamical systems. The sliding surface design problem is reduced to the specification of the desired time constant of closed-loop systems. The proposed scheme is able to accomplish a non-overshoot transient response and a short settling time for multivariable systems. The resulting sliding surfaces are robust and optimal in the existence of parameter perturbations. An integral sliding mode control approach is also developed for robust tracking by using the coefficient ratio-based robust sliding surface designs. The developed methods are implemented on a flexible robotic manipulator and a strike aircraft system, and the numerical simulation results are provided in order to show the validity and feasibility of the methods.

1 Introduction

Sliding mode control (SMC) is designed to drive state trajectories of a dynamical system onto a user defined sliding surface in the state space and to achieve sliding mode that provides reduced-order system dynamics, linearisation, and disturbance rejection (robustness) features. A sliding surface has a vital role in an SMC design since it determines the closed-loop system behaviour. A proper design of the sliding surface attains the control aims, for example, stability, response, tracking and regulation. Many industrial systems, for example, robotic and electro-mechanical systems, require a non-overshoot response and a quick response time. In the SMC, these requirements must be met with proper sliding surface designs.

Many sliding surface design approaches have been proposed over the last three decades. Some of these approaches are LQR-based design [1, 2], eigenstructure assignment [3], LMI-based design [4], H_2-based cost-sliding surface [5], geometric design [6], fuzzy sliding surface [7], a Lyapunov approach [8], zero-placement approach [9], time-varying surface [10–12], Ackerman's formula-based approach [13], moving sliding surfaces [14, 15] and non-linear sliding surfaces [16, 17]. The eigenstructure assignment and LQR-based methods have been successfully used to design sliding surfaces in recent years. However, many of the above methods cannot achieve the desired settling time and require complex procedures. Some of them are applicable to only single-input systems, and non-linear sliding surfaces are not unique mathematically and not applicable to multi-input systems.

This work proposes efficient, systematic, robust, and optimal sliding surface design algorithms for high control performances. An integral sliding mode control (ISMC) method with the proposed coefficient ratio-based sliding surface is also proposed for robust tracking. Coefficient ratios of sliding surfaces are directly defined from the desired settling time of closed-loop systems. Coefficient ratios have various forms, including Butterworth-type forms [18, 19], Kessler [20], Bessel [21] and standard form [22], which are obtained from experiments and practical implementations. In this work, the practicality, optimality, and robustness of the standard form are directly used in sliding surface designs in order to obtain desired stability, response, and robustness characteristics for closed-loop systems. Sliding surfaces ascertain short settling time and non-overshoot transient responses with the proposed coefficient ratio-based approaches.

The paper is organised as follows. A brief description of coefficient ratios of Hurwitz polynomials is given in Section 2. The procedures for designing sliding surfaces for multivariable systems are given in Section 3. An ISMC method is represented in Section 4. Section 5 provides applications of the proposed sliding surface and ISMC approaches to the flexible robot and aircraft systems. Finally, Section 6 presents the conclusion of the study.

2 Coefficient ratios of Hurwitz polynomials

Using sufficient stability conditions for Hurwitz polynomials can be a quick method for determining robust stability of many practical applications without doing computations in detail. Let a polynomial be

$$P(\lambda) = \sum_{i=0}^{r} a_i \lambda^i = a_r \lambda^r + \cdots + a_1 \lambda + a_0 \qquad (1)$$

where all real coefficients are either positive $a_i > 0$ or negative $a_i < 0$ for $i = 0, 1, \ldots, r$. $P(\lambda)$ is a Hurwitz polynomial if and only if all of its roots lie in the open left-hand side of the complex plane. The other method to check sufficient conditions for stability of Hurwitz polynomials is given by Lipatov and Sokolov conditions [23]

$$a_{i-1}a_{i+2} \leq 0.4655 a_i a_{i+1}, \quad i = 1, \ldots, r-2 \tag{2}$$

Besides, the sufficient condition for instability is

$$a_{i-1}a_{i+2} \geq a_i a_{i+1} \text{ for some } i,\ 1 \leq i \leq r-2 \tag{3}$$

An extension of the above sufficient conditions to robust Hurwitz polynomials was given in [24] as follows: let

$$a_i \in [\sigma_i, \delta_i], \quad \delta_i \geq \sigma_i > 0 \tag{4}$$

Then, the interval polynomial $P(\lambda)$ given in (1) and (4) is Hurwitz for all $a_i \in [\sigma_i, \delta_i]$, if

$$\delta_{i-1}\delta_{i+2} \leq 0.4655 \sigma_i \sigma_{i+1}, \quad i = 1, \ldots, r-2 \tag{5}$$

The stability conditions of the Hurwitz polynomials, given in (2) and (5), are simply the ratio of the consecutive coefficients of (1). Let γ_i be a coefficient ratio of the consecutive coefficients

$$\gamma_i = a_i^2/(a_{i-1}a_{i+1}), \quad i = 1, \ldots, r-1 \tag{6}$$

where $(a_{i-1}a_{i+2})/(a_i a_{i+1}) = 1/(\gamma_i \gamma_{i+1})$. Then, it is obvious from (6) and the condition (2) that the Hurwitz polynomial (1) is stable if all coefficient ratios γ_i are greater than 1.5 (or $\sqrt{\gamma_i \gamma_{i+1}} > 1.4657$). This implies that coefficient ratios can be predetermined. It is possible to consider the existing forms of coefficient ratios, for example, Butterworth [19], Kessler [20], Bessel [21], standard form [22], and k-polynomial [18, 19], in order to determine the coefficients of polynomial (1). For example, a simple and effective standard form of coefficient ratios with respect to stability and response requirements was recommended by Manabe [22] as

$$\gamma_1 = 2.5,\ \gamma_i = 2, \quad i = 2, \ldots, r-1 \tag{7}$$

Owing to simplicity and good response (non-overshoot) characteristics, the above standard form can be used to determine the coefficients of the Hurwitz polynomial (1). It is shown in [19] that the standard form (7) gives about 3τ settling time for an equivalent time constant τ, which characterises the speed of a closed-loop system with the characteristic polynomial $P(\lambda)$. The time constant τ is determined from the settling time t_{ss} requirement of a feedback system.

It should be noted that the coefficient ratios could always be adjusted to satisfy specific design requirements. In such cases, the stability conditions of the polynomial (1) must be satisfied.

3 Sliding surface design

SMC meets control design requirements with a proper sliding surface design. A quick, effective, and robust sliding surface can be designed with coefficient ratios of Hurwitz polynomials described in Section 2. To start design of sliding modes, first consider an uncertain dynamical system

$$\dot{z} = Az + Bu + Bf(z, u) \tag{8}$$

where $z \in \mathcal{R}^n$, $u \in \mathcal{R}^m$, $A \in \mathcal{R}^{n\times n}$, $B \in \mathcal{R}^{n\times m}$ with $1 \leq m \leq n$, and $f(z, u)$ contains bounded system uncertainties. It is assumed that B has full rank without loss of generality. For the system (8), let the sliding surface $s : \mathcal{R}^n \to \mathcal{R}^m$ be a linear function of states represented as

$$s(z) = Cz \tag{9}$$

where $C \in \mathcal{R}^{m\times n}$ is of full rank. If an SMC signal u drives the system states on the sliding surface (9) in a finite time t_s and maintains them on this surface thereafter, then an ideal sliding motion takes place in the system (8), that is, $s(z) = \dot{s}(z) = 0$ for all $t > t_s$. From the solution of $\dot{s}(z) = 0$, an equivalent control, which is necessary to maintain the states on the sliding surface, is defined by

$$u_{\text{eq}} = -(CB)^{-1}[CAz - f(z, u)] \tag{10}$$

Substituting the equivalent control (10) into (8) gives, for all $t > t_s$ and $Cz(t_s) = 0$

$$\dot{z} = \left(I_n - B(CB)^{-1}C\right)Az \tag{11}$$

which shows that the sliding motion is independent of control, but depends completely on the choice of the sliding surface. Although it is not clear how to design a suitable matrix C to achieve a specific control aim, it can be done by first transforming the system into a suitable regular form.

Suppose that the matrix pair (A,B) in the system (8) is controllable. Then, there exists a coordinate transformation $x = T_r z$ with $T_r \in \mathcal{R}^{n\times n}$ so that system (8) can be represented with the following regular form

$$\dot{x}_1 = A_{11}x_1 + A_{12}x_2 \tag{12}$$

$$\dot{x}_2 = A_{21}x_1 + A_{22}x_2 + B_2 u + f_2(x) \tag{13}$$

where $x_1 \in \mathcal{R}^{n-m}$, $x_2 \in \mathcal{R}^m$, $u \in \mathcal{R}^m$, $A_{11} \in \mathcal{R}^{(n-m)\times(n-m)}$, $A_{12} \in \mathcal{R}^{(n-m)\times m}$, $A_{21} \in \mathcal{R}^{m\times(n-m)}$, $A_{22} \in \mathcal{R}^{m\times m}$, $B_2 \in \mathcal{R}^{m\times m}$ and $f_2 \in \mathcal{R}^m$ is the bounded uncertainty vector. It is assumed that the matrix A_{12} and B_2 has full rank, that is, $\text{rank}(A_{12}) = m$, $\text{rank}(B_2) = m$ and $m \leq (n-m)$. The transformation matrix T_r can be found from the QR factorisation which satisfies $T_r B = [0\ B_2]^T$ [25].

A sliding surface for the system in the regular form (12) and (13) can be designed as

$$s(x) = C_1 x_1 + x_2 = \begin{bmatrix} C_1 & I_m \end{bmatrix} \begin{bmatrix} x_1 \\ x_2 \end{bmatrix} \tag{14}$$

where $C_1 \in \mathcal{R}^{m\times(n-m)}$ and the identity matrix $I_m \in \mathcal{R}^{m\times m}$. Once a sliding motion is established with a suitable control law, then during sliding mode $s(x) = 0$. Thus, expressing x_2 by means of x_1 in (14) results in $x_2 = -C_1 x_1$ and substituting for x_2 in (12) leads to the $n-m$ reduced-order system dynamics

$$\dot{x}_1 = (A_{11} - A_{12}C_1)x_1 \tag{15}$$

The matrix pair (A_{11}, A_{12}) is controllable since (A,B) is controllable [26]. Thus, the matrix $C_1 \in \mathcal{R}^{m\times(n-m)}$ can properly be designed in order to stabilise the reduced-order system. In addition to the stabilisation, the desired response of the feedback system must be ensured by the sliding surface.

3.1 Method 1: coefficient ratio-based robust eigenstructure assignment

The main goal of the coefficient ratio-based sliding surface design is to find a feedback gain C_1 whose eigenvalues are optimal and insensitive to perturbations as much as possible. By considering the foundations provided in Section 2, the desired time constant of the closed-loop system can be used to obtain the desired dynamics of the feedback system (12) and (13). For a given settling time t_{ss}, the equivalent time constant of the closed-loop system is equal to $\tau = t_{ss}/3$, which is the result of the use of the standard form

$$\gamma_1 = 2.5,\ \gamma_i = 2, \quad (i = 2, \ldots, n-m-1) \tag{16}$$

To use the standard form (16) in the sliding surface design, the characteristic polynomial of the closed-loop system (15) can be written as

$$|\lambda I - (A_{11} - A_{12}C_1)| = \sum_{i=0}^{n-m} \beta_i \lambda^i \tag{17}$$

with

$$\begin{aligned} &\beta_0 = 1, \quad \beta_1 = \beta_0 \tau, \\ &\beta_i = \beta_0 \tau^i / (\gamma_{i-1}^1 \ldots \gamma_1^{i-1}), \quad i = 2, \ldots, n-m \end{aligned} \tag{18}$$

where τ is the desired time constant of the system. Now, (17) has a set of desired optimal eigenvalues $\lambda = \{\lambda_1, \lambda_2, \ldots, \lambda_{n-m}\}$. These desired eigenvalues can be used in the robust eigenstructure assignment algorithm to determine sliding surfaces.

Let v_i and w_i be the right and left eigenvectors of the matrix $M = A_{11} - A_{12}C_1$, that is

$$Mv_i = \lambda_i v_i, \quad w_i^{\mathrm{T}} M = \lambda_i w_i^{\mathrm{T}} \tag{19}$$

If M has $n-m$ linearly independent eigenvectors, the sensitivity of an eigenvalue λ_i to perturbations in system matrices A_{11}, A_{12} and C_1 depends on the magnitude of the condition number c_i

$$c_i = \|w_i\| \|v_i\| / |w_i^{\mathrm{T}} v_i| \geq 1 \tag{20}$$

The condition number is a measure of the orthogonality of eigenvectors, that is, the corresponding condition number becomes smaller with increasing orthogonality of eigenvectors. Therefore a bound on the sensitivities of eigenvalues is given by [27]

$$\max(c_i) \leq \kappa(V) = \|V\| \left\|V^{-1}\right\| \tag{21}$$

where $\kappa(V)$ is the condition number of the matrix $V = [v_1, v_2, \ldots, v_{n-m}]$ of right eigenvectors. Now, using definitions (19)–(21), a robust eigenstructure assignment problem can be formulated. Given A_{11}, A_{12} and the set of desired optimal eigenvalues $\lambda = \{\lambda_1, \lambda_2, \ldots, \lambda_{n-m}\}$, find that the real matrix C_1 and non-singular matrix V satisfy

$$(A_{11} - A_{12}C_1)\, V = V\Lambda \tag{22}$$

where $\Lambda = \mathrm{diag}\{\lambda_1, \lambda_2, \ldots, \lambda_{n-m}\}$. A solution to (22) as C_1 exists if and only if [28]

$$U_1^{\mathrm{T}}(A_{11}V + V\Lambda) = 0 \text{ for } A_{12} = \begin{bmatrix} U_0 & U_1 \end{bmatrix} \begin{bmatrix} Z \\ 0 \end{bmatrix} \tag{23}$$

with $U = [U_0\ U_1]$ orthogonal and Z non-singular. Then C_1 is given by

$$C_1 = Z^{-1} U_0^{\mathrm{T}} \left(A_{11} - V\Lambda V^{-1}\right) \tag{24}$$

In the above algorithm, while V can always be chosen to be orthogonal for $m = n$ such that $c_i = 1$ for all i, an appropriate choice of V must be selected for general multivariable systems. Kautsky *et al.* [28] have developed a method that solves robust eigenstructure assignment problem in three steps:

Step 1: QR factorisation of A_{12} to find U_0, U_1, Z and construct an orthonormal bases

$$\left(U_1^{\mathrm{T}} (A_{11} - \lambda_i I)\right)^{\mathrm{T}} = \begin{bmatrix} \bar{S}_i & S_i \end{bmatrix} \begin{bmatrix} R_i \\ 0 \end{bmatrix}, \quad i = 1, 2, \ldots, n-m \tag{25}$$

Step 2: Select vectors $v_i = S_i e_i$ with $\|v_i\| = 1$, $i = 1, 2, \ldots, n-m$, such that $V = [v_1, v_2, \ldots, v_{n-m}]$ is well-conditioned. By iteration, each vector v_i is replaced by a new vector and this new vector is obtained by the QR factorisation

$$V_i = [v_1, v_2, \ldots, v_{n-m}] = \begin{bmatrix} Q_i & q_i \end{bmatrix} \begin{bmatrix} \bar{R}_i \\ 0^{\mathrm{T}} \end{bmatrix} \tag{26}$$

where $Q_i \in \mathcal{R}^{(n-m)\times(n-m-1)}$, $\bar{R}_i \in \mathcal{R}^{(n-m-1)\times(n-m)}$ and $q_i \in \mathcal{R}^{n-m}$ orthogonal to $\Gamma_i = \mathrm{span}(v_j, j \neq i)$. The vector q_i is then projected into S_i to give

$$v_i \equiv S_i e_i = S_i \frac{S_i^{\mathrm{T}} q_i}{\left\|S_i^{\mathrm{T}} q_i\right\|} \tag{27}$$

The iteration is continued until the reduction in $\kappa(V)$ is less than some positive tolerance.

Step 3: Find matrix $M = A_{11} - A_{12}C_1$ by solving $MV = V\Lambda$ and compute C_1 from $C_1 = Z^{-1}U_0^{\mathrm{T}}(A_{11} - M)$.

The optimality and robustness of the standard form (coefficient ratios), and the robustness of the eigenstructure assignment method are combined to design sliding surfaces. The design procedure of the proposed sliding surface method can be summarised with the following algorithm:

Algorithm 1 (Sliding surface design):

1. Get τ from a given settling time t_{ss} such that $\tau = t_{ss}/3$.
2. Calculate a transformation matrix T_r from the QR factorisation, which transforms the system (8) into the regular form (12) and (13).
3. Write the characteristic polynomial (17) of the desired spectrum of $A_{11} - A_{12}C_1$ by using the coefficients (18) and coefficient ratios γ_i (16). Then, obtain the desired optimal eigenvalues $\lambda = \{\lambda_1, \lambda_2, \ldots, \lambda_{n-m}\}$.
4. Finally, calculate the matrix C_1 with the robust eigenstructure assignment approach, and obtain the sliding surface (9) by $C = [C_1\ I_m]T_r$ for the original system (8).

3.2 Method 2: coefficient ratio-based direct sliding surface design

With a coordinate transformation $x_{11} = P^{-1}x_1$ for a non-singular transformation matrix P, (12) can then be written

doi: 10.1049/iet-cta.2014.0138

in a controllable canonical form

$$\dot{x}_{11} = P^{-1}A_{11}Px_{11} + P^{-1}A_{12}x_2 \tag{28}$$

where it is assumed that $\text{rank}(A_{12}) = m$. Here, the state x_2 can be considered as control input such that $x_2 = -G_1Px_{11}$. Then the system (28) turns out to be

$$\dot{x}_{11} = P^{-1}\left(A_{11} - A_{12}G_1\right)Px_{11} \tag{29}$$

With the selection of $G_1 = A_{12}^{\dagger}\left(A_{11} - L\right)$, the (29) becomes

$$\dot{x}_{11} = P^{-1}LPx_{11} \tag{30}$$

where $L \in \mathcal{R}^{(n-m)\times(n-m)}$ is the desired spectrum, and $A_{12}^{\dagger}$ is the Moore-Penrose inverse (Since $\text{rank}(A_{12}) = m$ and $m \leq (n-m)$, the Moore-Penrose inverse can be calculated as $A_{12}^{\dagger} = (A_{12}^{\mathrm{T}}A_{12})^{-1}A_{12}^{\mathrm{T}}$.) of A_{12} (i.e. $A_{12}^{\dagger}A_{12} = I_m$, where I is the unit matrix). By considering Section 2, the desired time constant of the closed-loop system can be used to obtain the desired dynamics of the feedback system (12) and (13). As explained in Section 2, for a given settling time t_{ss}, the equivalent time constant of the system is defined by $\tau = t_{ss}/3$, when the standard form of coefficient ratios $\gamma_1 = 2.5, \gamma_i = 2$ for $i = 2, \ldots, n-m-1$ is used. The characteristic polynomial of $\dot{x}_{11} = P^{-1}LPx_{11}$ can then be written as

$$\left|\lambda I - P^{-1}LP\right| = \sum_{i=0}^{n-m}\beta_i\lambda^i \tag{31}$$

where

$$\begin{aligned}&\beta_0 = 1, \quad \beta_1 = \beta_0\tau,\\ &\beta_i = \beta_0\tau^i/(\gamma_{i-1}^1\ldots\gamma_1^{i-1}), \quad i = 2,\ldots,n-m\end{aligned} \tag{32}$$

Here, the desired spectrum $P^{-1}LP$ has a canonical form

$$P^{-1}LP \equiv \Gamma = \begin{bmatrix}0 & 0 & \cdots & 0 & -\beta_0/\beta_{n-m}\\ 1 & 0 & \cdots & 0 & -\beta_1/\beta_{n-m}\\ 0 & 1 & \cdots & 0 & -\beta_2/\beta_{n-m}\\ \vdots & \vdots & \ddots & \vdots & \vdots\\ 0 & 0 & \cdots & 1 & -\beta_{n-m-1}/\beta_{n-m}\end{bmatrix} \tag{33}$$

Since $L = P\Gamma P^{-1}$, it is obvious that G_1 can be calculated from

$$G_1 = A_{12}^{\dagger}\left(A_{11} - P\Gamma P^{-1}\right) \tag{34}$$

This sliding surface design algorithm can be summarised as follows:

Algorithm 2 (Method 2):

1. Find τ from a given settling time t_{ss} as $\tau = t_{ss}/3$.
2. Calculate a transformation matrix P, to transform the first variable of the reduced-order system (12) into a controllable canonical form.
3. Write the characteristic polynomial of the desired spectrum $P^{-1}LP$ as in (31) by using the coefficients β_i (32) and coefficient ratios γ_i (16). Then, the desired spectrum $P^{-1}LP$ has the canonical form (33).
4. Finally, calculate the matrix G_1 using (34). For the original system (8), the sliding surface matrix is then $C = [G_1 I_m]T_r$.

3.3 Assessments of the proposed methods

If A_{12} is a square, non-singular matrix, then $A_{12}^{\dagger} = A^{-1}$. In this case Method 2 is equivalent to Method 1 (i.e. the reduced-order system has the same eigenvalues for both methods). If A_{12} is not a square matrix, then $A_{12}^{\dagger}$ has some properties of A^{-1}, and for this reason, Method 2 may not yield as effective results as Method 1. Furthermore, unlike Method 1, Method 2 requires a second transformation matrix which makes calculations complex for high-order systems. For these reasons, Method 1 is recommended in the sliding surface designs. For comparison, consider a simple example system

$$\begin{bmatrix}\dot{z}_1\\ \dot{z}_2\\ \hline \dot{z}_3\end{bmatrix} = \left[\begin{array}{cc|c}0 & 1 & 0\\ 0 & -2 & 1\\ \hline 0 & 0 & -1\end{array}\right]\begin{bmatrix}z_1\\ z_2\\ \hline z_3\end{bmatrix} + \begin{bmatrix}0\\ 0\\ \hline 10\end{bmatrix}u \tag{35}$$

where the system output is $y = z_1$. For an equivalent time constant $\tau = 1$ s, the sliding surface matrix is found as $C = \begin{bmatrix}-2.5 & -0.5 & -1\end{bmatrix}$ for Method 1, and $C = \begin{bmatrix}-1 & 0 & -1\end{bmatrix}$ for Method 2. It is clear that system (35) is in the regular form. By considering the partitioned system matrices, the matrix $A_{12} = [0 \quad 1]^T$ is not a non-singular square matrix, so the Method 1 and Method 2 are not equivalent. In numerical simulations, the SMC law is taken as $u = -(CB)^{-1}[CAz + k_1\,\text{sign}(s)]$ with $k_1 = 5$ and the saturation function (see (45)) is used instead of the sign$(\cdot)$ function.

Fig. 1 illustrates the performance of the SMC under sliding surface algorithms, Method 1 and Method 2. The SMC gives different results for these different algorithms. Method 1 yields a settling time $t_{ss} \simeq 3$ s, while Method 2 ends up with a settling time $t_{ss} \simeq 6$ s. In addition, the control signal of the SMC under these sliding surfaces is also completely different. The gain k_1 of the SMC law does not have any effect on the settling time, and the performance of Method 2 can only be improved with different time constants (e.g. a smaller τ for the given example).

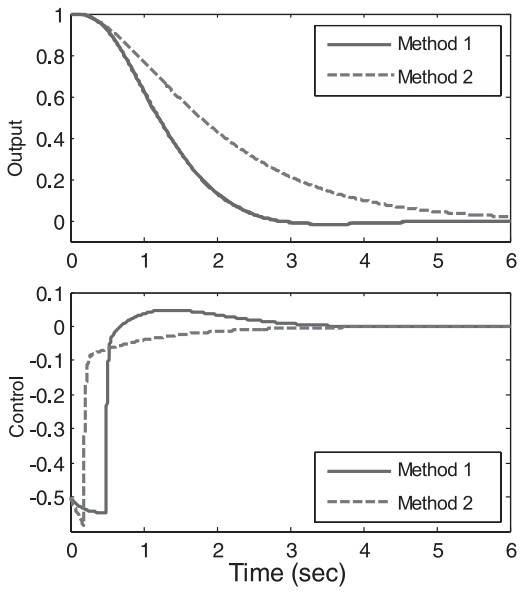

Fig. 1 *Performance comparison of the proposed sliding surface algorithms*

Table 1 Basic features of the coefficient ratio-based sliding surface design method

	LQR	Pole placement	Coefficient ratio (Method 1)
design	1 difficult to obtain desired roots 2 trial-error is necessary to obtain weight matrix Q	1 arbitrarily and manually pole selection to obtain sliding surfaces	1 automatic pole assignment from coefficient ratios 2 only desired time constant is required to design sliding surface
optimality:	optimal	non-optimal	near-optimal
robustness:	non-robust	robust	robust

The coefficient ratio-based method combines advantages of LQR and pole placement (eigenstructure assignment)-based approaches as depicted in Table 1. In the LQR-based sliding surface designs, one needs to determine a weight matrix through trial-and-error approach to find suitable eigenvalues for the reduced-order system and to solve the Riccati equation. In pole placement approach, the eigenvalues of the reduced-order system are arbitrarily assigned (except for the dominant eigenvalue), which results in non-optimal sliding surfaces. On the other hand, the coefficient ratio-based approach needs only the desired settling time of the system, which simplifies the design and produces near-optimal sliding surfaces.

Robustness of the coefficient ratio-based sliding surfaces can be assessed similarly as those given for robust Hurwitz polynomials [24]. Assume that the system matrices in (13) have some small perturbations ΔA_{11} and ΔA_{12}, then we have

$$\dot{x}_1 = ((A_{11} + \Delta A_{11}) - (A_{12} + \Delta A_{12})C_1)x_1 \tag{36}$$

Owing to the perturbations, the characteristic polynomial of (36) can be represented similar to (24) with

$$\beta_i \in [\alpha_i, \delta_i], \quad \delta_i > \alpha_i > 0 \tag{37}$$

Theorem 1 [24]: The interval polynomial $P(\lambda)$ of the system (36) defined in (1) and (37) is Hurwitz for all $\beta_i \in [\alpha_i, \delta_i]$ if

$$\delta_{i-1}\delta_{i+2} \leq 0.4655\alpha_i\alpha_{i+1}, \quad (i = 1, \ldots, n-m-2) \tag{38}$$

For proof of the theorem, see [24].

In addition, the robustness of the pole placement algorithm has been shown by Kautsky *et al.* [28]. Consequently, the optimal transient response characteristics [19, 22, 29] and the robustness of coefficient ratios [24], and the robustness of eigenstructure assignment method [28] are combined in the coefficient ratio-based sliding surface design. Disturbance rejection and robustness capability of the proposed approach is illustrated in Section 5.1.

4 Integral sliding mode control for robust tracking

Tracking control is an inevitable part of control systems. Since integral control allows obtaining robust tracking of reference signals, it will be utilised in the SMC design. Although there exist some ISMC approaches [30–35], a coefficient ratio-based ISMC procedure can be simpler and more effective.

By augmenting the plant states (8) with integral states, the following state-space representation can be obtained

$$\dot{x}_a = A_a x_a + B_a u + B_a f(x_a, u) - B_r r \tag{39}$$

with

$$x_a = \begin{bmatrix} \sigma \\ z \end{bmatrix}, \quad A_a = \begin{bmatrix} 0 & H \\ 0 & A \end{bmatrix}, \quad B_a = \begin{bmatrix} 0 \\ B \end{bmatrix}, \quad B_r = \begin{bmatrix} I_p \\ 0 \end{bmatrix} \tag{40}$$

where integral states $\sigma \in \mathcal{R}^p$, tracking signals $r \in \mathcal{R}^p$, and H is the output matrix of the system (i.e. $y = Hz$ where y is the system output). The augmented system is controllable if the pair (A,B) is controllable and [36]

$$\text{rank} \begin{bmatrix} A & B \\ H & 0 \end{bmatrix} = n + p \tag{41}$$

Now, the ISMC procedure for the augmented system (39) can be explained as follows. Define an augmented state-dependent sliding surface

$$s(x_a) = Cx_a \tag{42}$$

Now, the sliding surface matrix C can easily be calculated by using augmented system matrices and the sliding surface design procedure described in Section 3. Once a sliding motion is established with a suitable SMC law, then we have $s(x_a) = \dot{s}(x_a) = 0$ during sliding mode. Such a suitable SMC law can be obtained by using equivalent control [37], sliding-sector control [38], and sliding mode order approach [39, 40], and it is necessary to achieve the reachability condition $s^T\dot{s} < 0$ and the sliding motion. For the augmented system (39), an equivalent control-based SMC law [37] from the solution of $\dot{s}(x_a) = 0$ can be obtained as

$$u = -(CB_a)^{-1}\left[CA_a x_a - CB_r r + k_1 \text{sign}(s)\right] \tag{43}$$

where k_1 is a constant gain and the sign(•) function is defined column-wise as $\text{sign}(s) = [\text{sign}(s_1) \ldots \text{sign}(s_m)]^T$ with $\text{sign}(s_i) = s_i/|s_i|$ for $i = 1, 2, \ldots, m$. The SMC law (43) must make the sliding surface a stable invariant set, $s(x_a) = 0$. By considering the augmented system (39), sliding surface (42), and control law (43), stability analysis of the ISMC can be done with the reachability condition as follows

$$\begin{aligned} s^T\dot{s} &= s^T(CA_a x_a + CB_a u + CB_a f - CB_r r) \\ &= s^T(CA_a x_a - CA_a x_a + CB_r r - k_1 \text{sign}(s) + CB_a f - CB_r r) \\ &= s^T(-k_1 \text{sign}(s) + CB_a f) \\ &\leq -(k_1 - \|CB_a f\|)\|s\| \end{aligned} \tag{44}$$

Since $f \equiv f(x_a, u)$ is assumed to be bounded, the reachability condition, $s^T\dot{s} < 0$, holds if $k_1 > ||CB_a f||$. Consequently,

doi: 10.1049/iet-cta.2014.0138

once a sliding motion occurs, the sliding surface determines dynamic behaviour of the feedback system, and the system response remains insensitive to matched uncertainties or disturbances in the sliding mode [37]. Note that the order of the motion equation is lower than or equal to the original system, and ISMC design procedure is the same as the conventional SMC.

5 Applications for robot and aircraft systems

Implementations of the proposed coefficient ratio-based sliding surface algorithm and the ISMC method will be illustrated on a flexible robotic manipulator and a strike aircraft system. Note that in the following applications, sign(·) function is approximated to saturation function to avoid chattering and to provide continuous control signals [12], that is, for a small $\varepsilon > 0$

$$\text{sign}(s_i) \approx \begin{cases} s_i/|s_i|, & \text{if} \quad |s_i| > \varepsilon \\ s_i/\varepsilon, & \text{if} \quad |s_i| \le \varepsilon \end{cases} \tag{45}$$

5.1 One-link flexible robotic manipulator

Consider a one-link flexible robotic manipulator [41]

$$\begin{aligned} \dot{z}_1 &= z_2 \\ J\dot{z}_2 &= \mu(z_3 - z_1) - bz_2 + u \\ \dot{z}_3 &= z_4 \\ I\dot{z}_4 &= \mu(z_1 - z_3) - \Omega \sin z_3 \end{aligned} \tag{46}$$

where the system states denote motor position z_1, motor velocity z_2, link position z_3, link velocity z_4 and y is the system output, $y = z_1$. The control u is the motor torque supply in the form of (43). The system parameters with appropriate units are spring stiffness $\mu = 2.25$, motor inertia $J = 0.0463$, viscous friction coefficient $b = 0.058$, gravitational torque $\Omega = 0.4$, and link inertia $I = 0.1154$. It is obvious that the non-linear term because of gravitational torques of the system (46) can be considered as an unmatched uncertainty.

To design the sliding surface matrix C, the desired setting time of the system is assumed to be $t_{ss} = 1.5$ s, which leads to an equivalent time constant of $\tau = 0.5$ s. By using Algorithm 1, the integral sliding surface matrix is found as

$$C = \begin{bmatrix} -102.56 & -20 & -1 & -31.28 & -3.99 \end{bmatrix} \tag{47}$$

and eigenvalues of the system are calculated as $\lambda = (-5 \pm 1.62i, -5 \pm 6.88i)$.

Numerical simulations are realised by using the MATLAB/Simulink programs in order to verify the performance of the proposed sliding surface algorithm and the ISMC. The control design parameters are chosen as $k_1 = 20$ and $\varepsilon = 0.01$, and initial conditions of the system are taken as $z(0) = (0.1, 0, 0, 0)$.

A simple performance comparison of the ISMC under optimal, eigenstructure assignment, and coefficient ratio-based sliding surfaces is illustrated in Fig. 2. To evaluate the disturbance rejection and robustness capabilities of the proposed approaches, it is assumed that there are 25% variations on the link inertia I and gravitational torque Ω, in addition to the unmatched uncertainty (the non-linear term of the system). The simulation results are given for maximum, nominal, and minimum values of the uncertain parameters. The design parameters of the coefficient ratio, optimal, and eigenstructure assignment-based sliding surfaces are selected as $\tau = 0.5$, $Q = \text{diag}(100, 10, 0.01, 10, 1)$, and $\lambda_i = \{-5 \pm 4i, -6, -7\}$, respectively. These parameters are carefully selected in order to obtain close results to the coefficient ratio-based approach. For the optimal sliding surface, it is seen from Fig. 2 that while settling time is satisfied, the sliding surface can escape from zero under the control gain $k_1 = 20$. However, it is possible to obtain good results for some other Q values (or larger control gains). It is obvious that the coefficient ratio-based method gives the best results for the given design parameters. The main advantage of the coefficient ratio-based approach is that it needs only one parameter, that is, the time constant of the system, while parameter selections of the optimal and eigenstructure assignment (pole placement) based approaches require some trial-and-error (i.e. some effort and time). In addition,

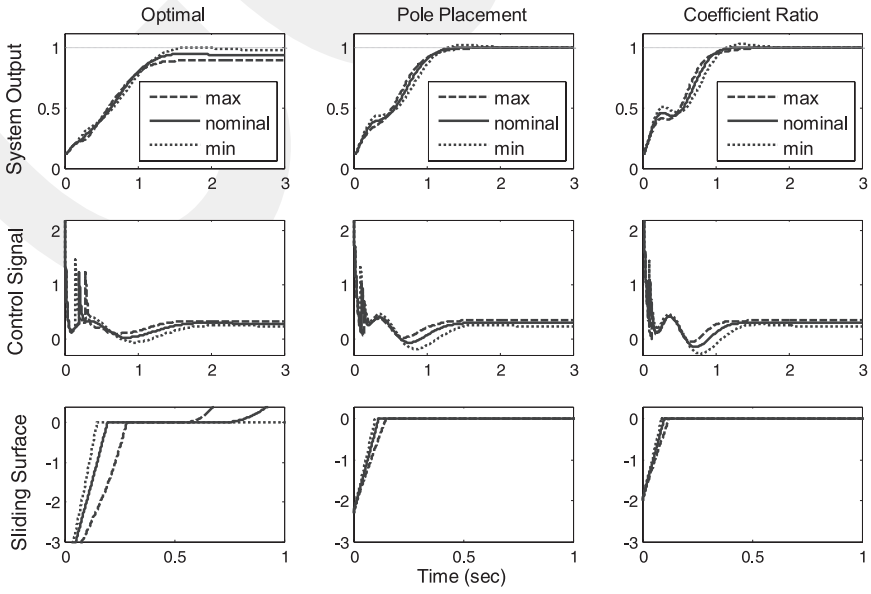

Fig. 2 *Robustness evaluation of the optimal, pole placement, and coefficient ratio-based sliding surface designs for the ISMC of the flexible robot by considering maximum (max), nominal and minimum (min) values of the system parameters*

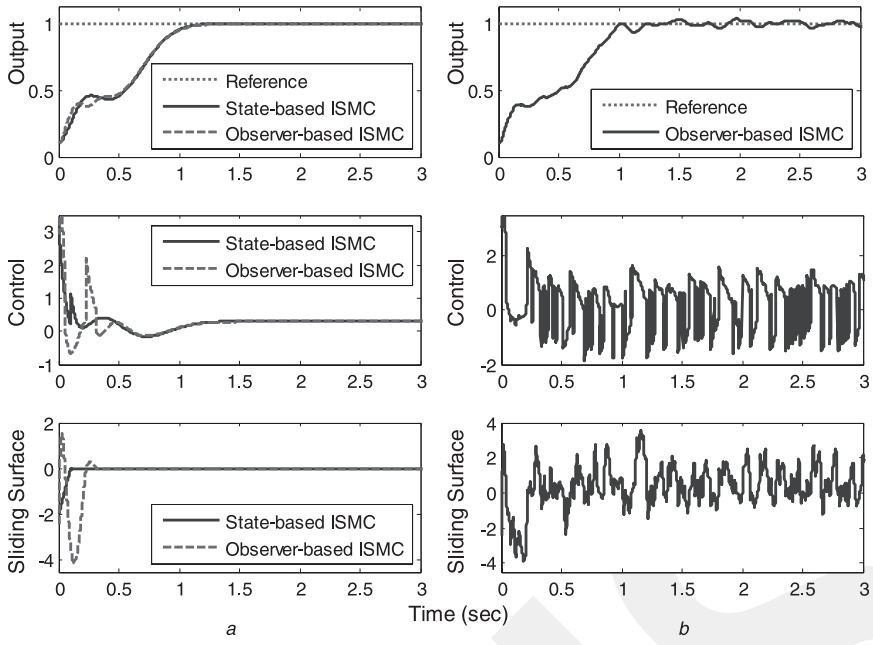

Fig. 3 *Time responses of the system output, sliding surface, and control signal of the integral sliding mode controlled one-link flexible robot*

a No noise
b Observer-based ISMC under noisy measurement

the coefficient ratio-based approach can provide the shortest reaching time and the least control energy. These results verify Table 1.

Fig. 3 shows the time responses of the system output, control signal and sliding surface. The settling time for the state variables is about $t_{ss} = 1.5$ s, which satisfies design requirements. The initial motion towards the sliding surface and a sliding motion along the line $s(z) \simeq 0$ occurs at around $t_s = 0.1$ s. Note that if the initial condition of the system is zero (or the system is initially in the equilibrium), then a sliding motion will occur from beginning of the time (i.e. the reaching phase will be eliminated). The performance of the ISMC is highly satisfactory with robust, non-overshoot transient response, and zero tracking error.

To implement state feedback control schemes in practice, the state variables must be available via either measurement or estimation. If all the state variables are not measurable, a full-state observer can simply be designed as

$$\dot{\hat{z}} = A\hat{z} + f(\hat{z}, u) + \psi(y - H\hat{z}) \tag{48}$$

where ψ is the observer gain matrix. The observer-based ISMC has larger transients because of having different initial conditions, but gives a satisfactory result. In Fig. 3*b*, the control performance is provided under noisy system measurement with an additive noise in the range of $\pm 10\%$ of the system output, and again a satisfactory performance is obtained. However, as seen from Fig. 3*b*, the observer-based ISMC under noisy measurements results in aggressive responses of the control signal and the sliding surface. Hence, a low level of the measurement noise is a significant factor for the success of SMC approaches.

5.2 Strike aircraft

The strike aircraft dynamics at Mach 0.85 and at a height of 12 km can be represented with the following model [42]

$$\begin{aligned}
\dot{z}_1 &= -z_1 + u_1 \\
\dot{z}_2 &= z_1 \\
\dot{z}_3 &= z_2 \\
\dot{z}_4 &= 0.09u_2 \\
\dot{z}_5 &= z_4 - z_5 \\
\dot{z}_6 &= -0.088z_1 + 0.0345z_2 + z_5 - 0.0032z_6
\end{aligned} \tag{49}$$

where the state variables denote vertical acceleration z_1, rate of change of height z_2, height z_3, thrust commanded z_4, change in thrust z_5 and change in airspeed z_6. To have a stable closed-loop system behaviour with a desirable performance, the control law ($u = [u_1, u_2]^T$) can be in the form of (43). By considering the condition (41), the augmented system matrix of the strike aircraft is controllable for the system outputs

$$y_1 = z_3, \quad y_2 = z_6 \tag{50}$$

The aircraft outputs, height y_1 and speed change y_2, must be held at some desirable references with the ISMC. The reference vector r is chosen to be $r = [100 \quad 0]^T$ initially, that is, the aircraft path requires a sudden step change in the terrain of 100 m and a constant speed, but then the height moves to 150 m and turns back to 100 m. To design the controller, the settling time of the system is taken as $t_{ss} = 6$ s, and thus the equivalent time constant is $\tau = 2$ s. Using the Algorithm 1, the sliding surface matrix C is calculated as (see (51))

$$C = \begin{bmatrix} -24.98 & 15.97 & -1 & -8.23 & -24.73 & 0 & 5.27 & 15.58 \\ -35.28 & -39.98 & 0 & -10.12 & -37.52 & -1 & -9.39 & -39.44 \end{bmatrix} \tag{51}$$

doi: 10.1049/iet-cta.2014.0138

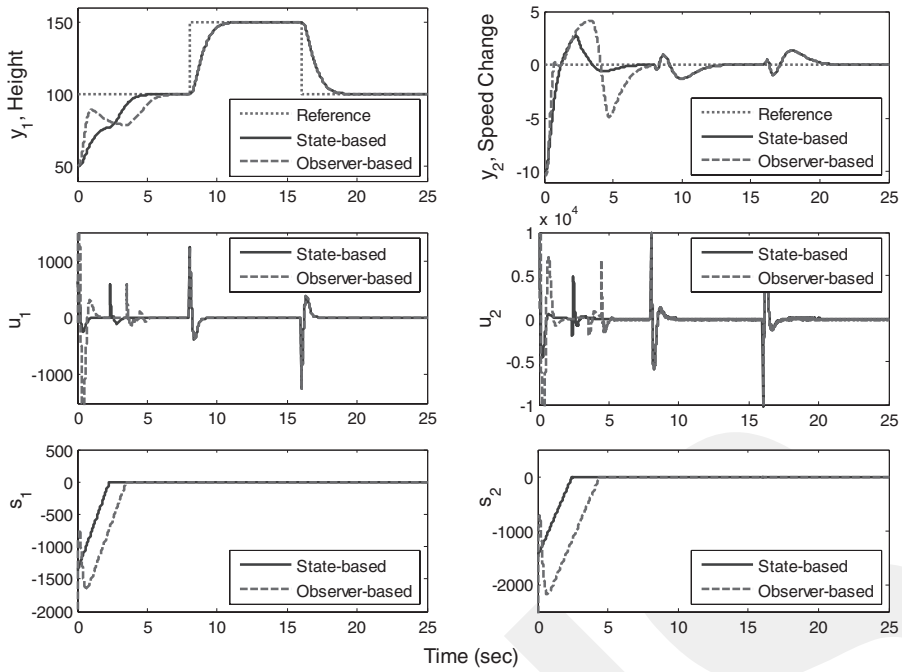

Fig. 4 *Time responses of the aircraft system under the ISMC for step height changes and constant speed references*

and the eigenvalues of the system are found as $\lambda = (-1.48, -1.6 \pm 0.93i, -4.16, -5.57 \pm 6.52i)$.

Numerical simulation results are shown in Fig. 4 for the control gain $k_1 = 500$ and $\varepsilon = 1$, and the initial condition $z(0) = (-10, 0, 50, 0, 0, -10)$. The time responses of the system outputs, control signals and sliding surfaces are displayed in Fig. 4. It is seen from Fig. 4 that the settling time is about $t_{ss} = 6$ s, and there is no overshoot, which ensures design specifications. Since all the state variables are not measurable, a full-state observer as described in (48) can be designed. Similar to the flexible robot application, the observer-based control initially causes larger transients because of having different initial conditions, but it provides the same performance with the state feedback design after initial reaching. That is, during the reference variations at 8th and 16th s, observer-based control is equal to the state feedback control when there is no noise in the measurements. Another significant result is that the ISMC eliminates the reaching phase during step reference changes, except for the initial reaching (if the system is not in the equilibrium initially).

6 Conclusion

Robust, optimal, and systematic sliding surface algorithms and an ISMC method are proposed for enhancing the performance of SMC systems. It is shown that with the coefficient ratio-based approach, the sliding surface design problem is reduced to the specification of the desired settling time of the closed-loop system. Based on the proposed coefficient ratio-based sliding surface approach, an ISMC method is also presented for robust tracking. Flexible robotic manipulator and aircraft applications show that robust, non-overshoot, and short settling time performances are achieved with the proposed methods. The methodologies can be used in any single or multivariable SMC systems to obtain superior performance. For practical implementations, an algorithm is also provided.

7 Acknowledgment

This work was supported by Turkish Scientific and Research Council (TUBITAK) under project no. 113E329.

8 References

1 Utkin, V.I., Young, K.: 'Methods for constructing discontinuity planes in multidimensional variable structure systems', *Autom. Remote Control*, 1978, **39**, pp. 1466–1470
2 Pan, Y., Furuta, K.: 'VSS controller design for discrete-time systems', *Control Theory Adv. Technol.*, 1994, **10**, (4), pp. 669–687
3 Dorling, C.M., Zinober, A.S.I.: 'Two approaches to hyperplane design in multivariable variable structure control systems', *Int. J. Control*, 1986, **44**, (1), pp. 65–82
4 Choi, H.H.: 'LMI-based sliding surface design for integral sliding mode control of mismatched uncertain systems', *IEEE Trans. Autom. Control*, 2007, **52**, (4), pp. 736–741
5 Takahashi, R., Peres, P.: 'H_2 Guaranteed cost-switching surface design for sliding modes with nonmatching disturbances', *IEEE Trans. Autom. Control*, 1999, **44**, (11), pp. 2214–2218
6 Elghezawi, O., Zinober, A.S.I., Billings, S.A.: 'Analysis and design of variable structure systems using a geometric approach', *Int. J. Control*, 1983, **38**, pp. 657–671
7 Lee, H., Kim, E., Kang, H., Park, M.: 'Design of a sliding mode controller with fuzzy sliding surfaces', *IET Control Theory Appl.*, 1998, **32**, (6), pp. 411–418
8 Su, W.C., Drakunov, S., Ozguner, U.: 'Constructing discontinuity surfaces for variable structure systems – a Lyapunov approach', *Automatica*, 1996, **32**, (6), pp. 925–928
9 Meza, M.E., Bhaya, A.: 'Zero-placement approach to the design of sliding surfaces for linear multivariable systems', *IET Control Theory Appl.*, 2001, **148**, (5), pp. 333–339
10 Bartoszewicz, A.: 'Time-varying sliding modes for second-order systems', *IEE Proc. Control Theory Appl.*, 1996, **143**, (5), pp. 455–462
11 Choi, S.-B., Park, D.-W., Jayasuriya, S.: 'A time-varying sliding surface for fast and robust tracking control of second-order uncertain systems', *Automatica*, 1994, **30**, (5), pp. 899–904
12 Slotine, J.-J.E., Li, W.: 'Applied nonlinear control' (Prentice Hall, 1991)
13 Ackermann, J., Utkin, V.I.: 'Sliding mode control design based on Ackermann's formula', *IEEE Trans. Autom. Control*, 1998, **43**, pp. 234–237
14 Park, D.-W., Choi, S.-B.: 'Moving sliding surfaces for high-order variable structure systems', *Int. J. Control*, 1999, **72**, (11), pp. 960–970

15 Roy, R.G., Olgac, N.: 'Robust nonlinear control via moving sliding surfaces-n-th order case', *IEEE Conf. Decis. Control*, 1997, **2**, pp. 943–948
16 Fulwani, D., Bandyopadhyay, B., Fridman, L.: 'Non-linear sliding surface: towards high performance robust control', *IET Control Theory Appl.*, 2012, **6**, (2), pp. 235–242
17 López-Martínez, M., Acosta, J.A., Cano, J.M.: 'Non-linear sliding mode surfaces for a class of underactuated mechanical systems [Brief Paper]', *IET Control Theory Appl.*, 2010, **4**, (10), pp. 2195–2204
18 Ben Hariz, M., Bouani, F., Ksouri, M.: 'Robust controller for uncertain parameters systems', *ISA Transactions*, 2012, **51**, (5), pp. 632–640
19 Kim, Y.C., Keel, L.H., Bhattachayya, S.P.: 'Transient response control via characteristic ratio assignment', *IEEE Trans. Autom. Control*, 2003, **48**, (12), pp. 2238–2244
20 Kessler, C.: 'Ein beitrag zur theorie mehrschleifiger regelungen', *Regelungstechnik*, 1960, **8**, (8), pp. 261–266
21 Manabe, S., Kim, Y.C.: 'Recent development of coefficient diagram method'. Asian Control Conf., Shanghai, China, 2000
22 Manabe, S.: 'Unified interpretation of classical, optimal, and Hinf control', *J. SICE*, 1991, **30**, (10), pp. 941–946
23 Lipatov, A.V., Sokolov, N.I.: 'Some sufficient conditions for stability and instability of continuous linear stationary systems', *Autom. Remote Control*, 1979, **39**, pp. 1285–1291
24 Bose, N.K., Jury, E.I., Zeheb, E.: 'On robust Hurwitz and Schur polynomials', *IEEE Trans. Autom. Control*, 1988, **33**, (12), pp. 1166–1168
25 Shtessel, Y.: 'Sliding mode control and observation' (Birkhäuser, New York, 2014)
26 Edwards, C., Spurgeon, S.K.: 'Sliding mode control: theory and applications' (CRC Press, 1998)
27 Wilkinson, J.H.: 'The algebraic eigenvalue problem' (Clarendon Press, Oxford University Press, Oxford, 1988)
28 Kautsky, J., Nichols, N.K., Van Dooren, P.: 'Robust pole assignment in linear state feedback', *Int. J. Control*, 1985, **41**, (5), pp. 1129–1155
29 Tavazoei, M.S., Haeri, M.: 'Comparison of the existing methods in determination of the characteristic polynomial', *World Acad. Sci. Eng. Technol*., 2005, **6**, pp. 130–133
30 Abidi, K., Xu, J.-X., Xinghuo, Y.: 'On the discrete-time integral sliding-mode control', *IEEE Trans. Autom. Control*, 2007, **52**, (4), pp. 709–715
31 Bejarano, F.J., Fridman, L.M., Poznyak, A.S.: 'Output integral sliding mode for min-max optimization of multi-plant linear uncertain systems', *IEEE Trans. Autom. Control*, 2009, **54**, (11), pp. 2611–2620
32 Comanescu, M.: 'An induction-motor speed estimator based on integral sliding-mode current control', *IEEE Trans. Ind. Electron.*, 2009, **56**, (9), pp. 3414–3423
33 Xu, J.-X., Guo, Z.-Q., Lee, T.H.: 'Design and implementation of integral sliding-mode control on an underactuated two-wheeled mobile Robot', *IEEE Trans. Ind. Electron.*, 2014, **61**, (7), pp. 3671–3681
34 Zhao, F., Liu, Y., Yao, X., Su, B.: 'Integral sliding mode control of time-delay systems with mismatching uncertainties', *J. Syst. Eng. Electron.*, 2010, **21**, (2), pp. 273–280
35 Utkin, V., Shi, J.: 'Integral sliding mode in systems operating under uncertainty conditions', Proc. 35th IEEE Conf. on Decision Control, 1996, vol. 4, pp. 4591–4596
36 Khalil, H.K.: 'Nonlinear systems' (Prentice Hall, 2002, 3rd edn.)
37 Utkin, V.I., Guldner, J., Shi, J.: 'Sliding mode control in electromechanical systems' (CRC Press, 2009, 2nd edn.)
38 Furuta, K., Pan, Y.: 'Variable structure control with sliding sector', *Automatica*, 2000, **36**, (2), pp. 211–228
39 Bartolini, G., Pisano, A., Usai, E.: 'Second-order sliding-mode control of container cranes', *Automatica*, 2002, **38**, (10), pp. 1783–1790
40 Levant, A.: 'Sliding order and sliding accuracy in sliding mode control', *Int. J. Control*, 1993, **58**, (6), pp. 1247–1263
41 Spong, M.: 'Modeling and control of elastic joint Robots', *ASME J. Dyn. Syst. Meas. Control*, 1987, **109**, pp. 310–319
42 McLean, D.: 'Automatic flight control systems' (Prentice-Hall, 1990)

doi: 10.1049/iet-cta.2014.0138